Available online www.jocpr.com

Journal of Chemical and Pharmaceutical Research, 2012, 4(5):2724-2732

Research Article

ISSN : 0975-7384
CODEN(USA) : JCPRC5

Structural investigations of Mn(II) doped in diaquacesiumdiaquabismalonatozincate using single crystal EPR study

Geetha. P[1], Parthipan. K[2], Sathya. P[2], Balaji. S[1]

[1]*SCSVMV University, Kanchipuram, Tamilnadu, India*
[2]*Department of Chemistry, Pondicherry University, Puducherry, India*

ABSTRACT

In the present studies spotlight on the structural investigation of Mn(II) doped diaquacesiumdiaquamalonatozincate (DCDMZ) carried out room temperature using single crystal EPR, UV-Visible, FT-IR and powder XRD techniques. Obtained EPR spectra result shows that 30 lines hyperfine patterns, it indicates manganese present in the host lattice. Angular variation of EPR spectra in the three orthogonal planes shows that presence of only one site having large D value, with orthogonal symmetry. The spin Hamiltonian parameter evaluated using three orthogonal crystal rotations are g_{xx} = 1.8586, g_{yy} = 2.0001, g_{zz} = 2.0641; A_{xx} = 8.30, A_{yy} = 9.04, A_{zz} = 9.20; D_{xx} = 5.48, D_{yy} = 18.89 and D_{zz} = -24.38 mT. The large zero field tensor due to steric interaction of Malonato Bridge. The direction cosines of metal ligand bond Zn-O did not matched with direction cosines obtained from EPR-NMR confirms that Mn(II) impurity present in zinc malonate lattice is in interstitial position. Observed optical spectra data shows the characteristics of Mn (II) ions in distorted octahedral symmetry.

Keywords: EPR, Hyperfine, Spin Hamiltonian, Crystal lattice, Admixture coefficient, Interstitial.

INTRODUCTION

Spectral and structural studies of transition metal containing carboxylate ligand have great attention for their potential application in the field crystal engineering, metal organic frame work, supramolecular behaviors, biological properties, molecular electronics, catalysis and molecular based magnetic materials [1,2]. From the coordination chemistry point of view, malonate is a good chelating versatile ligand and it exhibit different configurations like syn-syn and anti-anti through one or both carboxylate group. In, addition carboxylate group provides an efficient pathway for coupling magnetic centre either ferromagnetic or antiferromagnetic[3-9]. In these kinds of systems, the coupling constant is influenced by structural factors such as the conformation of bridged or the geometry of the metal environment. Single crystal EPR, is the only technique, gives more information about symmetry, defect and covalence of metal ligand bond. EPR technique is used to study paramagnetic ions in diamagnetic and paramagnetic host lattices to understand phase transitions, defects, orientation effects, covalence of the metal-ligand bond, relaxation times, symmetry etc[10-17]. The probability of gathering information from magnetically concentrated system is vanished due to very broad resonances, arising from dipolar-dipolar interaction. Hence, to understand the symmetry and covalence around the embedded ion, generally paramagnetic ions are doped either in diamagnetic or paramagnetic host lattices of known symmetry. In the past few years, our research group has been concentrating on the transition metal ions doped diamagnetic malonato complexes. Our focus on diaquacesiumaquabismalonatozincate is extended, because this is very interesting host lattice which holds alkali metal as well as transition metal. Single crystal EPR studies also exposes the location of paramagnetic impurity, i.e., interstitial, substitutional or both. In this view, we select diaquacesiumaquabismalonatozincate (here after abbreviated as DCDMZ) as good host to incorporate Mn(II) as dopant that has been undertaken to find the spin Hamiltonian parameters, the location of dopant, structural and bonding parameters.

EXPERIMENTAL SECTION

Single crystals of manganese doped DCDMZ was prepared by literature procedure [18]. Solid zinc carbonate had been added to an aqueous solution of malonic acid, which was kept under stirring. These solutions were stirred for 30 min and followed by refluxing on water bath. At this stage, 0.1% by weight of manganese sulphate was added as dopant. An aqueous solution (10 ml) of cesium carbonate (0.116 g, 1 mmol) was added gradually to the above reaction mixture with continuous stirring and refluxing. After half an hour, the reaction mixture was cooled down to the room temperature [18]. The resulting solution was allowed to stand at room temperature. After couple of weeks, as a result, good and well shaped crystals were separated out from the solution.

2.1 EPR Studies

The EPR spectra were recorded at room temperature on a JEOL JES-TE100 ESR spectrometer operating at X-band frequencies, having a 100 kHz field modulation to obtain the first derivative EPR spectrum. DPPH was used as the standard for magnetic field correction and for g-factor calculations. Angular variation was made at room temperature by rotating the crystal along the three mutually orthogonal planes a, b, c* in at 10º intervals. An Isofrequency plot of each plane was simulated using EPR-NMR program. The EPR spectrum of the powder sample was simulated using Simfonia program developed and supported by Bruker Biospin.

2.2 Optical Absorption

Optical spectrum of Mn doped DCDMZ was recorded at room temperature using a Varian Cary 5000 Ultraviolet (UV-Visible) near infrared spectrophotometer in the region of 200-1200 nm**.**

2.3 FTIR and Powder XRD Studies

FTIR spectrum of manganese doped DCDMZ was recorded at room temperature. In our present study, the FTIR spectra was recorded on a Shimadzu FTIR -8300/8700 spectrometer, 4cm^{-1} resolution, automatic gain, 20 scan, in the region of 4000-400 cm^{-1}. The measurements were made using almost transparent KBr pellets containing fine powder sample at room temperature. In the crystalline material, the powder X-ray diffraction pattern (XRD) was used to identify, characterize and confirm the powder sample possessing long and short range orders respectively. In the present investigation, the powder XRD was carried out with doped and undoped materials on a PANalytical Xpert Pro diffactometer with Mn kα radiation of wavelength 0.15406 nm and 2θ values of 5-75°.

3. Crystal Structure

Diaquacesiumaquabismalonatozincate is abbreviated as DCDMZ with molecular formula $C_6H_{12}Cs_2Zn_1O_{12.}$ DCDMZ is iso-structured with $C_6H_{12}Cs_2Cu_1O_{12}$ and belongs to a triclinic crystal class with space group $P\bar{1}$, having unit cell parameters a = 0.71166, b = 0.71316, c = 0.75211 nm and α = 87.33 º, β = 79.42º γ = 86.69 º and Z = 1 [18]. The structure of DCDMZ is made up of $[Zn(mal)_2(H_2O)_2]^{2-}$ anion and $[Cs(H_2O)]^+$ cations which is attracted by hydrogen bond thus leading to 3D network. Two complexes have two metal atoms namely zinc and cesium. Zinc atom coordinates with six oxygen atoms; four among them are carboxylate oxygen atoms from two different malonate carboxyl groups and two oxygens from water molecule and thus exhibits an elongated octahedral geometry. The cesium atom is eight coordinated thus exhibits a highly distorted square antiprism environment. Two water molecules and two carboxylate malonate oxygen atoms build one basal plane of the square antiprism. The other basal plane of the squre antiprism, which was four carboxylate oxygen atoms from three different malonate groups, was slightly distorted. The structure of the DCDMZ is shown in Fig 1.

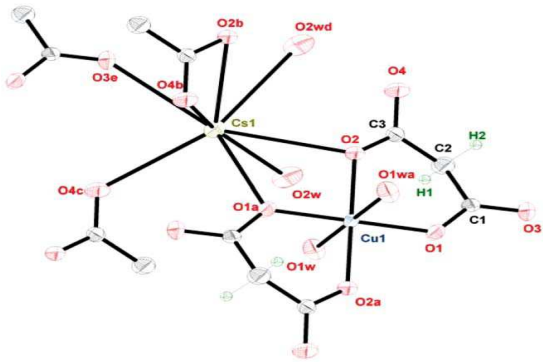

Fig 1: Molecular packing diagram for DCDMZ [18]

The optical adsorption spectrum was recorded at room temperature and shown in Fig 2a. The optical absorption studies of manganese doped DCDMZ shows two bands at 42 735 and 15 649 cm^{-1}. The strong band has been

observed in the range of 42 735 cm^{-1} and which is assigned as charge transfer band, which usually occurs in the range of 35 000-50 000 cm^{-1}. Another broad band at 15 649 cm^{-1} is an attribute of the manganese ion in tetragonal distorted octahedral symmetry. According to this, the broad band is assigned for the transition between $^2B_{1g}$ - $^2B_{2g}$. Using the above mentioned transition, we have calculated tetragonal distortion parameter (Dq) 10Dq = 15 649 cm^{-1}[19].

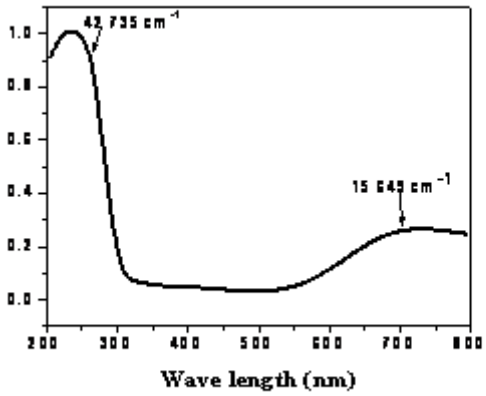

Fig 2a: Powder optical absorption spectrum of Mn(II) doped DCDMZ at room temperature.

The FTIR spectrum of Mn (II) doped DCDMZ is recorded at room temperature is shown in Fig 2b. The band observed at 1655 cm^{-1} is responsible for carboxylate (COO^-) symmetrical stretching and the bands observed around at 3436 cm^{-1} and 3105 cm^{-1} are owed for O-H bending corresponding to water ligand. Three bands are noticed at 975, 788 and 732 cm^{-1} corresponding to the bending modes of O-C-O bond. The band observed at 1445 cm^{-1} corresponds to C=C stretching. However, this spectrum is supportive to confirm that there is no structural changes has been taken place after doping DCDMZ with small amount of Mn(II) impurity.

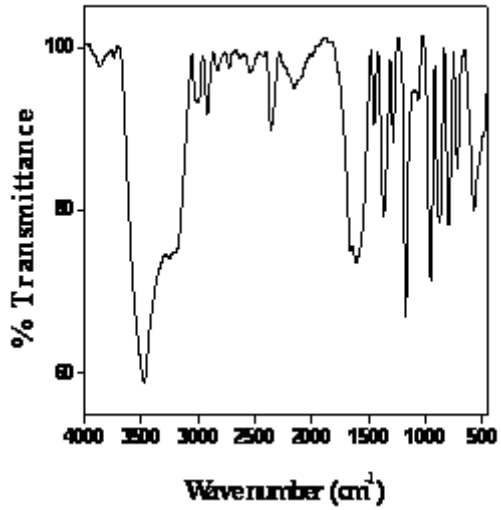

Fig 2b: The FTIR spectrum of Mn (II) doped DCDMZ

The powder XRD pattern of Mn (II) doped DCDMZ and pure DCDMZ have been recorded at room temperature is shown in Fig 2c. Crystal lattice parameters a, b, c for manganese doped DCDMZ and pure DCDMZ have been calculated from powder XRD. These values are same and resemble the reported value of DCDMZ and it confirms that the formation of lattice DCDMZ. Moreover the low concentration of manganese impurity does not alter structure.

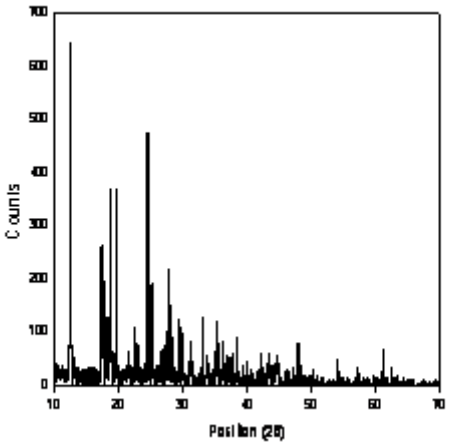

Fig 2c: Powder XRD pattern of Mn(II) doped DCBZ

4.1 EPR Studies

Manganese ion has $3d^5$ electronic configuration with $^6S_{5/2}$ ground state (based on Hund's rule). In crystalline field low symmetry, the ground state splits into three Kramers doublet specially ±1/2, ±3/2 and ±5/2. In the applied magnetic field, the degeneracy is completely eliminated and it gives rise to five fine structure transitions. Each line will be further split-up into six hyperfine lines, totally it gives 30 lines. The observed single crystal EPR spectrum of Mn(II) doped DCDMZ in a*c*plane are shown in Fig 3a, where the crystal c* axis is parallel to applied magnetic field. Single crystal EPR measurements of Mn(II) doped DCDMZ shows well separated 30 hyperfine line patterns. Lines are occurred due to the coupling of electron S = 5/2 (electron spin) of manganese, with its nuclear spin I = 5/2 and it clearly says that only one site present in the lattice. Because the unit cell have one molecule (Z=1) there is no other way to enter into another site. This same phenomenon has been monitored for vanadyl and copper doped DCDMZ. Two more EPR spectra are given in Fig 3b and Fig 3c for ab and bc* planes respectively with their respective orientations. Single crystals of optimum size have been chosen for EPR rotation. Selected crystal has been mounted into the EPR cavity rotate at 10˚ difference at room temperature. Any system with total electron spin of 5/2 will give rise to only one EPR line, in the absence of zero-field splitting. In the absence of applied magnetic field, the ground state of Mn(II) ion $^6S_{5/2}$ splits into three Kramer's' doublets with separations of 4D and 2D due to electron-electron interaction. During crystal rotation most of the planes gives 30 line patterns it's due to the electro spin of Manganese S =5/2 and I = 5/2. The observed spectrum clearly shows five transitions namely -5/2 - -3/2, -3/2 - -1/2. -1/2 – 1/2, ½- 3/2 and 3/2- 5/2. Transitions between these levels will give rise to five equally spaced lines, each of them will further split-up into a sextet due to hyperfine interaction from the nuclear spin of ^{55}Mn (I = 5/2). Hence a five set pattern of six components each (i.e., 30 line pattern) is expected. Characteristic EPR spectra at 300 K, when the applied magnetic field (B) is parallel to axis a, axis b and axis c*, are shown in Figures 7.4a, 7.4b and 7.4c respectively. Angular variation plots of hyperfine lines in the three orthogonal planes ac*, bc* and ab are drawn from observed. Angular variation plots are shown in the fig 4a-4c, in these figures, solid circle represents the experimental values whereas the continuous straight line represents simulated values obtained using EPR-NMR program.

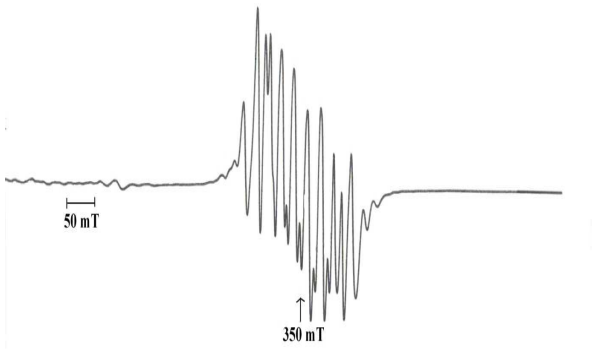

Fig 3a: Single crystal EPR spectrum of Mn(II) doped DCDMZ recorded, when A parallel to axis c. Frequency = 9.06849 GHz.

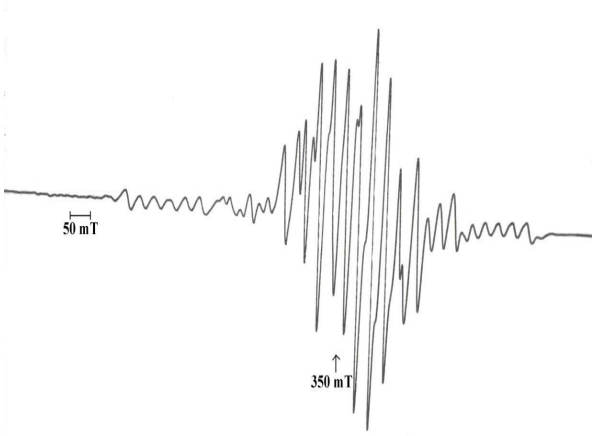

Fig 3b: Single crystal EPR spectrum of Mn(II) doped DCDMZ, when B is parallel to the axis c*. Frequency = 9.06856 GHz

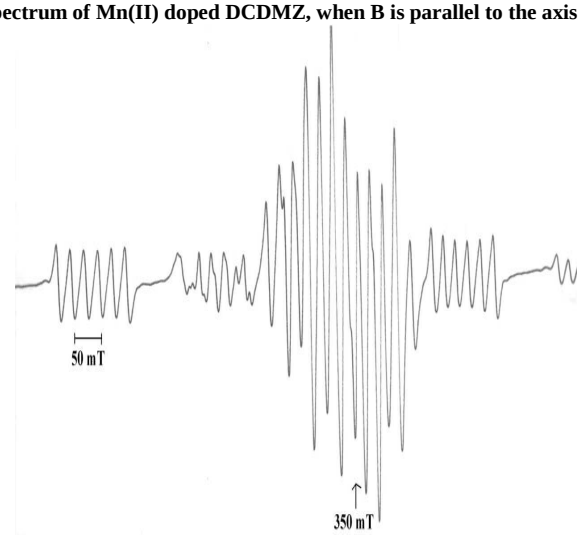

Fig 3c: Single crystal EPR spectrum of Mn (II) doped DCDMZ, when applied magnetic field (B) is parallel to axis a. Frequency = 9.07554 GHz.

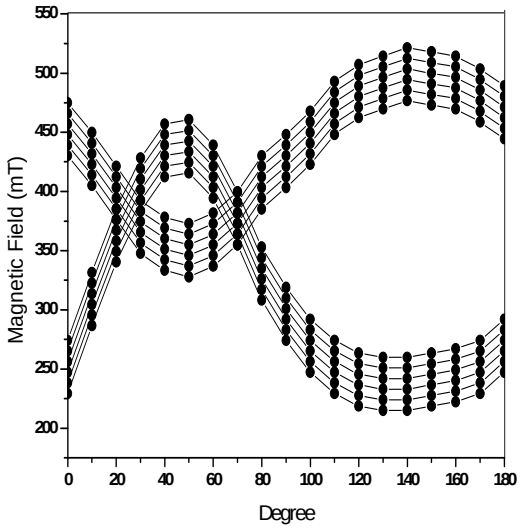

Fig 4a: Angular variation plots of Mn (II)/DCDMZ in a*c*plane at room temperature. Here θ = 140˚ corresponds to the c* axis and θ = 50˚ corresponds to the crystallographic axis.

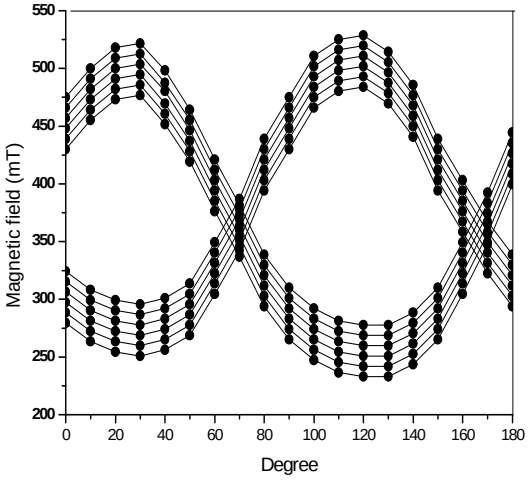

Fig 4b: Angular variation plots of Mn (II)/DCDMZ in bc* plane at room temperature. Here θ = 40˚ corresponds to the c* axis and θ = 50˚ corresponds to the crystallographic b axis. υ = 9.06856 GHz

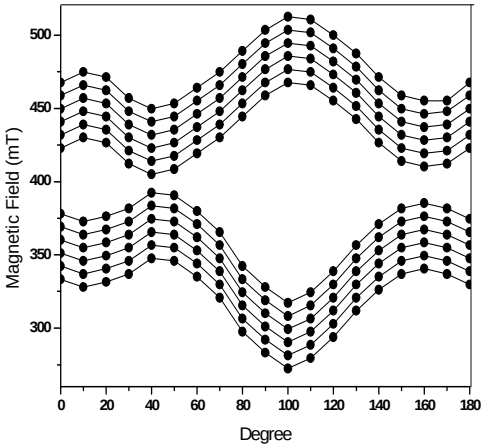

Fig 4c: Angular variation plots of Mn (II)/DCDMZ in ab plane at room temperature. Here θ = 0˚ corresponds to the a* axis and θ = 80˚ corresponds to the crystallographic b axis. υ = 9.07554 GHz

4.2 Calculation of spin-Hamiltonian parameters

All the observed transitions are fitted to the following spin Hamiltonian parameters.

$$\mathcal{H}s = g_{xx}\beta B_x S_x + g_{yy}\beta B_y S_y + g_{zz}\beta B_z S_z + A_{xx}S_x I_x + A_{yy}S_y I_y + A_{zz}\, S_z I_z$$

Here, first term represents the Zeeman energy, and the second term is due to hyperfine interaction. The axial and rhombic components of the zero fields splitting are represented by the third and fourth terms. S_x, S_y, S_z are the spin operators with respect to the cubic field axes. The parameters D and E are zero fields splitting due to rhombic and axial crystalline field matrix and E represents the deviation from the axial symmetry. Using the above equation spin Hamiltonian parameters is calculated, shown in Table-2 along with respective direction of cosines. From Table-1 without a doubt it shows that g/A/D is nearly coincident, and additionally we know that the geometry of Mn(II)/DCDMZ distorted octahedral symmetry. The value of D is relatively higher than for normal Mn(II) complexes. In order to identify the position of the Mn in DCDMZ, the direction cosines of various Zn-O bonds have been calculated using X-ray data (assuming similar structure for DCDMZ) and given in Table-2. Location of dopant has been identified by direction cosines. By comparison of direction cosines are obtained from EPR-NMR program and direction cosines values calculated from crystal X-ray, if both the values match with each other [20]. It indicates that the dopant present in the lattice is in substitution way, but the values are dissimilar with each other, it signifies that dopant present in the lattice is in interstitial position. The calculated values of direction cosines for the present case are shown in Table-1 and 2, and it clearly says that dopant present in the lattice intestinally instead of substitution due to steric nature of malonate ligand. Orientation of the dopant has been discussed below. The road maps are also simulated for all the three planes, good agreement have been obtained. The spin Hamiltonian

parameters observed from single crystal analysis are further confirmed by taking polycrystalline EPR spectrum. The powder EPR spectrum of Mn(II)/ DCDMZ is shown in Fig.5. The calculated spin Hamiltonian parameters are: g = 2.0078, A = 9.6 and D = 52.24 mT. These values are almost close to those parameters acquired from single crystal analysis. The powder EPR spectrum is simulated using these values which confirm the accuracy of the evaluated spin Hamiltonian parameters is shown in Fig.5.

Principle values				Direction cosines		
g matrix				a	b	c*
1.9789	0.000	-0.1012	2.000	-0.7082	0.2216	0.6808
	2.000	0.000	1.8586	-0.5816	0.7012	0.4126
		1.9438	2.000	-0.3596	0.6795	0.6471
A matrix (mT)						
8.56	0.00	-5.07	8.32	0.0001	0.7218	-0.6919
	9.20	0.00	8.54	1.000	0.000	0.000
		8.51	9.74	0.006	-0.6919	-0.7219
D matrix (mT)						
7.22	0.00	-14.8	18.89	0.0000	1.000	0.000
	18.69	0.00	5.49	0.7579	0.000	0.6523
		-11.7	-24.38	-0.6523	0.0002	0.7579

Table 1: Spin Hamiltonian Parameters obtained from the single crystal rotations for Mn(II) in DCDMZ using program EPR-NMR [19]

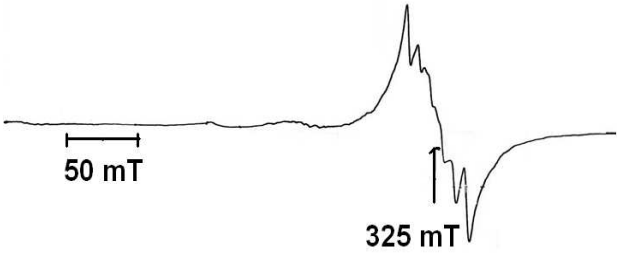

Fig 5: Powder EPR spectrum of Mn (II) doped DCDMZ recorded at RT (Top) whereas bottom one simulated using simfonia program. Frequency = 9.08161 GHz

Table 2: The direction cosines of Zn –O bonds in DCDMZ obtained from the crystallographic data [18].

M-L bond	Direction cosines		
	a*	b*	c*
Zn-O1m	0.1438	-08278	0.4894
Zn-O2m	0.1653	0.4314	0.8874
Zn-O_w	0.9051	0.4195	0.0688

Orientation of the Mn(II) ions in the lattice: The location of the paramagnetic impurity site observed for Mn (II) doped in DCDMZ is interstitial. We have analyzed crystal structure of DCDMZ depicted in Fig1. DCDMZ posses one molecule per unit cell (Z = 1) under the space group $P\bar{1}$. Zinc atom coordinates with six oxygen, four from two different malonate groups builds the equatorial plane and two oxygen from two symmetrical water molecule made of elongated octahedral geometry. Cesium atom is eight coordinated with square antiprism environment [18]. For the present case dopant ion is manganese and it is preferred to replace host zinc ion because both have comparable ionic radii and same oxidation state. But not privileged to replace cesium atom because it is univalent ion. The $3d^5$ ion with s =5/2 and I = 5/2 exhibits 30 line hyperfine pattern from a Mn (II) doped DCDMZ single crystal. Mn(II) ion has been planned to enter in the host lattice interstitially because both metal atoms (Zn and Cs) are strongly coordinated with malonate bridge and also breaking of metal ligand bonds (Zn-O and Cs-O) is very difficult. Suppose zinc atom coordinates with six water molecule, it is very easy to replace by dopant manganese ion but present system is very complicated due to carboxylate group. Spin Hamiltonian parameters are good agreement with literature values [21-22]

4.3. Covalency of metal ligand bonds:

The covalence of the bond between manganese and oxygen ligand can be calculated using matumura's plot. The covalence of a bond between manganese and its ligands depends on the magnitude of the isotropic hyperfine coupling constant "A". An approximate relationship for the covalency of a bond between the atom p and q and their electro negativities χ_p and χ_q is given [**20**].

$$C = [1 - 0.16(\chi_p-\chi_q)-0.035(\chi_p-\chi_q)^2]/n$$

Here, n is the number of neighboring atoms surrounding the Mn(II) ion. Using the values χ_{Mn} = 1.55 and χ_{O} = 3.44, (Pauling's scale) and the percentage of covalency obtained for our case using the above equation is 8.5%, indicating that compound is almost ionic in nature. Also, the covalency of the bond between manganese and its ligands will influence the magnitude of the isotropic hyperfine coupling constant. The hyperfine coupling constant A is obtained from Matamoras's plot matches well with the calculated value [21-24].

CONCLUSION

Structural studies on Mn(II) doped DCDMZ has been successfully performed at room temperature. FTIR and powder XRD data support the confirmed formation of lattice DCDMZ and also finalize the presence of dopant do not alter the structure of host lattice due to low concentration. Single crystal rotation in the three planes indicates that only one site is noticed for manganese impurity that is present in DCDMZ lattice. The spin Hamiltonian parameters for the Mn (II) doped DCDMZ have been calculated from single crystal rotation in the three orthogonal planes. The principal g, A and D values are evaluated using EPR-NMR program. The spin Hamiltonian parameters have been calculated and direction cosines values confirm that the impurity has entered the lattice in an interstitial position. The large D and E values reveals the distortion present in the crystal lattice due to steric effects of the malonic acid in the lattice. The isofrequency plots and the powder EPR have also been simulated, which are used in the evaluation of spin Hamiltonian parameters.

Acknowledgements

The authors thank the University Grand Commission [33-316/2007(2007)] for financial assistance. PG dedicates this paper to (Late) Dr. P. Sambasiva Rao for his valuable guidance in the research work. PG acknowledges the Principal and the management, Rajiv Gandhi College of Engineering and Technology, Pondicherry for the support.

REFERENCES

[1] B. Hue, M. Liang Tong, X. M. Chen, *Coord. Chem. Rev.*, **2005**, 249, 545-565.
[2] C. Ruiz-Perez, Y. Rodriguez-Martin, M. Hernandez-Molina, F. S. Delgado, J. Pasan, J. Sanchiz, F. Lloret, M. Julve, *Polyhedron*, **2003**, 22, 2111-2123.
[3] J. Pasan, F. S. Delgado, Y. Rodriguez-Martin, M. Hernandez-Molina, C. Ruiz- Perez, J. Sanchiz, F. Lloret, M. Julve, *Polyhedron*, **2003**, 22, 2143-2153.
[4] C. Oldham, in: G. Wilkinson, R.D. Gillard, J.A. McCleverty (Eds.), Comprehensive Coordination Chemistry, Pergamon Press, Oxford, U.K, **1987**, 2,435-8.
[5] R. Hoskins, R. Robson, *J. Am. Chem. Soc*., **1990**, 112, 1546-1554.
[6] G. B. Gardner, D. Venkataraman, J.S. Moore, S.Moore *Nature* **1995**, 374, 792-795.
[7] D. Chattopadhya, S. K. Chttopadhyay, P. R. Lowe, C. H. Schwalbe, S. K. Mazumder, A. Rana, S. Ghosh, *J.Chem.Soc.,Daltan Trans*., **1993**, 913-918.
[8] S. Kitagawa, S. Noro, T. Nakamura, *Chem. Commun*., **2006**, 39, 701-707.

[9] D. Reinen, M. Atanasov, P. Kohler, D. Babel, *Coord. Chem. Rev*., **2010**, 254, 2703-2754.
[10] B.J. Hathaway, G.Wilkinson, Comprehensive Coordination Chemistry. Pergamon press, New York **1987**, 5, Chap 53.
[11] B. J. Hathaway, D. E. Billing, *Coordination. Chem*., **1970**, 5, 143-207.
[12] N. Wei, N. N. Murthy, K. D. Karlin, *Inorg. Chem*., **1994**, 33, 6093-6100.
[13] M. Velayutham, B. Varghese, S. Subramanian, *Inorg. Chem*., **1998**, 37, 5983-5991.
[14] G. A. Mclachlan, G.A. Fallon, R. L. Martin, L.Spiccia, *Inorg. Chem*., **1995**, 34, 254-261.
[15] P. Comba, T. W. Hambley, M. A. Hitchman, H. Stratemeier, *Inorg. Chem*., **1995**, 34, 390-396.
[16] J. G. Lozano, J. S. Carrio, E. Escriva, J. V. Foldado, C. Molla , L. Lezama, *Polyhedron*, **1997**, 16, 939-956.
[17] D. Reinen, C. Friebel, *Inorg. Chem*., **1984**, 23, 791-799.
[18] F. S. Delgado, C. R. Perez, J. Sanchiz, F. Llret, M. Julve, *Cryst Engcom*m., **2006**, 8, 507-512.
[19] F.Clark, R.S. Dickson, D.B.Fulton, J. Isoya, A. Lent, D.G. McGavin, M.J Mombourquette, R. H. D. Nuttal, P. S. Rao, H.Rinnerberg, W.C. Tennat, J.A. Weil, EPR –NMR program. University of Saskatchewan, Saskatoon, Canada **1996**
[20] O.Matamur, *J. Phys. Soc. Jpn*., **1959**, 14, 108-116.
[21] S. Boobalan, P. Sambasiva Rao, *J. Organo. Chem*., **2010**, 695, 963-969.
[22] S. Boobalan, P. Sambasiva Rao, *Radiat. Eff. Defects Solids*., **2010**, 38, 25-37
[23] H. Ramesh, K. Parthipan, P. Sambasiva Rao, *Appl.Mag.Reson*., **2011**, 40, 513-524.
[24] P. Geetha, K. Parthipan, P. Sambasiva Rao, *Appl Magn Reson*., **2012**, 42, 187-196.